

Two-current model of the composition dependence of resistivity in amorphous $(\text{Fe}_{100-x}\text{Co}_x)_{89-y}\text{Zr}_7\text{B}_4\text{Cu}_y$ alloys using a rigid-band assumption

S. Shen,¹ P. R. Ohodnicki,² S. J. Kernion,¹ and M. E. McHenry¹

¹*Department of Materials Science and Engineering, Carnegie Mellon University, Pittsburgh, Pennsylvania 15213, USA*

²*Chemistry and Surface Science Division, National Energy Technology Laboratory (NETL), Pittsburgh, Pennsylvania 15236, USA*

(Received 13 June 2012; accepted 12 October 2012; published online 21 November 2012)

Composition dependence of resistivity is studied in amorphous $(\text{Fe}_{100-x}\text{Co}_x)_{89-y}\text{Zr}_7\text{B}_4\text{Cu}_y$ ($0 \leq x \leq 50$, $y = 0, 1$) alloys. The two-current model proposed by Mott for crystalline materials is extended to a disordered amorphous system where s-d scattering is dominant in electron conduction. A rigid-band assumption is made due to the small atomic number difference between Fe and Co. Band structures with a constant density of states (DOS), parabolic distributed DOS, and Gaussian distributed DOS were investigated to fit experimental data. The Gaussian distributed DOS was found to simulate the resistivity maximum and magnetic moment maximum in the Fe-rich region. The basic concepts presented here can potentially provide insight into the optimization of FeCo-based HITPERM alloys for applications at increased frequencies. © 2012 American Institute of Physics. [<http://dx.doi.org/10.1063/1.4765673>]

I. INTRODUCTION

Electrical conduction in ferromagnetic transition metals was modeled by Mott¹ considering two independent parallel currents, carried by spin-up and spin-down electrons. The two-current model applies below the Curie temperature, T_c when scattering events that conserve spin directions are more probable. Above T_c , spin-mixing effects limit application of the two-current model. This model has been used to discuss the anisotropic magnetoresistance in Fe-containing amorphous alloys.² We extend the two-current model, as originally proposed for crystalline materials, to consider the composition dependence of resistivity in ferromagnetic amorphous FeCoZrBCu alloys with high T_c 's. The resistivity variation in the transition from Fe with unfilled 3d majority spin band to Co with fully filled 3d majority spin band is related to the density of 3d states. A resistivity minimum which occurs in binary crystalline FeCo alloys is eliminated in this disordered alloy system because, like lower dimensional systems,³ the localization of d-states and band narrowing results in smaller compositional region with weak ferromagnetism.

Since unoccupied d-states determine both scattering of the s-conduction electrons into the d-band (s-d scattering) and ferromagnetism in transition metals, electrical resistivity and magnetic moment (Slater-Pauling curve) are determined by band structures. A simple rigid-band model originally proposed by Friedel⁴ can account for some variations in physical properties observed on alloying. In the rigid-band model, the s- and d-bands are assumed to be rigid in shape with changing atomic number. This simplifies modeling band filling by shifting the Fermi level (E_F) through the bands according to the number of electrons present. Due to the small difference in atomic number between Fe and Co, it is appropriate to apply the rigid-band model to the amorphous FeCoZrBCu alloys investigated here.

Amorphous alloys reported here are based on Fe-rich HITPERM being studied for high temperature power conversion applications. HITPERM (original composition, $\text{Fe}_{44}\text{Co}_{44}\text{Zr}_7\text{B}_4\text{Cu}_1$) is a nanocomposite alloy with large T_c 's of both the amorphous and nanocrystalline phases after crystallization due to Co substitution for Fe.⁵ Since increasing resistivity of the amorphous matrix in nanocomposites is important for reducing eddy current losses at high frequencies, understanding its composition dependence in the amorphous precursor of HITPERM can potentially lead to the development of nanocomposite materials with lower losses for high frequency applications.⁶ After crystallization, HITPERM alloy exhibits a microstructure consisting of α' -FeCo nanocrystallites (B2 structure) embedded in an amorphous matrix. We use the band structure for bcc Fe(Co) to estimate the density of states (DOS) of the amorphous alloys investigated here, assuming they are not significantly different from that of the thermodynamically favored crystalline phase.⁷

II. EXPERIMENTAL RESULTS

Amorphous alloys of nominal compositions $(\text{Fe}_{100-x}\text{Co}_x)_{89-y}\text{Zr}_7\text{B}_4\text{Cu}_y$ ($0 \leq x \leq 50$, $y = 0, 1$) were prepared by melt-spinning. As-cast ribbons were ~ 3 mm wide and 20–30 μm thick. The resistivity of each ribbon 300 mm in length was calculated from dc resistance and average cross-sectional area. A Grainger Exttech 380560 High Resolution Milliohm Meter was used to measure dc resistance at room temperature ($T \ll T_c$) by a 4-point probe method. Densities were measured by the Archimedes method for calculating an average cross-sectional area.

Fig. 1 shows a maximum resistivity to occur at a Fe:Co ratio around 75:25 (dashed line). In comparison, Beitel and Pugh⁸ showed the composition dependence of resistivity in bulk crystalline FeCo alloys to have a maximum at 10 at. % of Co followed by a minimum due to chemical ordering at

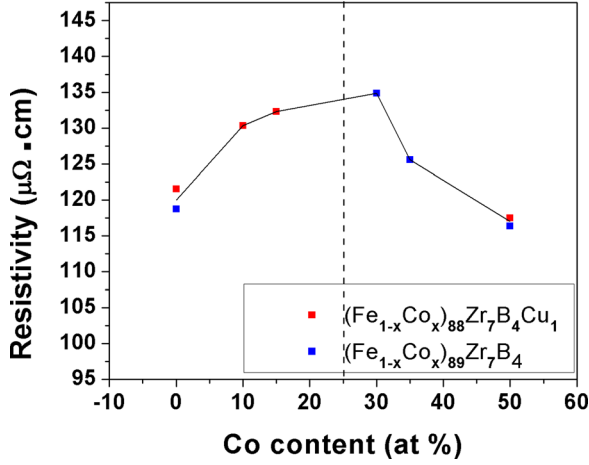


FIG. 1. Composition dependent resistivity of amorphous $(\text{Fe}_{100-x}\text{Co}_x)_{88-y}\text{Zr}_7\text{B}_4\text{Cu}_y$ ($0 \leq x \leq 50$, $y = 0, 1$) alloys.

intermediate compositions. Therefore, the disordered amorphous $(\text{Fe}_{100-x}\text{Co}_x)_{89-y}\text{Zr}_7\text{B}_4\text{Cu}_y$ ($0 \leq x \leq 50$, $y = 0, 1$) alloys we investigated in this work are appropriate for studying spin-down strong ferromagnetism.

III. DISCUSSIONS

A. Two-current model

In this section, the two-current model by Mott will be briefly introduced and applied to the alloy system of concern in this work where the resistivity is mainly due to s-d scattering. Fig. 2 shows this model to consider electron conduction in ferromagnetic transition metals as a parallel circuit with resistivity from two types of carriers. These are, respectively, spin-up (represented by ρ^\uparrow) and spin-down electrons (represented by ρ^\downarrow). ρ^\uparrow is not necessarily equal to ρ^\downarrow because of the difference of the DOS between spin-up and spin-down subbands at E_F . Below T_c , the overall resistivity can be expressed as

$$\rho = \frac{\rho^\uparrow \cdot \rho^\downarrow}{\rho^\uparrow + \rho^\downarrow}. \quad (1)$$

The resistivity of each channel can be expressed by the simple Drude model for free electrons

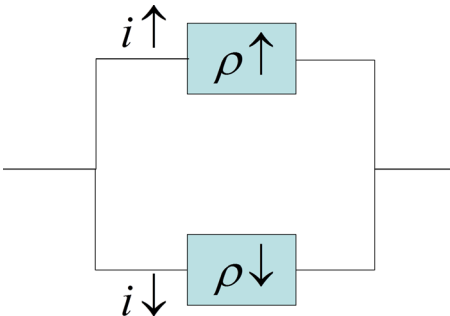


FIG. 2. The two-current model of the electron conduction in ferromagnetic transition metals.

$$\frac{1}{\rho^\uparrow \downarrow} = \sigma^\uparrow \downarrow = \frac{ne^2\tau}{m^*}, \quad (2)$$

where σ is the conductivity, n is the volume concentration of free carriers, e is the electronic charge, τ is the relaxation time, and m^* is the effective mass of the charge carriers. m^* is inversely proportional to the band curvature. In transition metals, the d-bands are much narrower than the s-bands which result in very large effective masses for the d-electrons. Thus, electrical conduction is almost entirely due to s-electrons in transition metals.

The relaxation time τ is related to the DOS at E_F available for s-d scattering

$$\tau^{-1} = |V_{scat}|^2 N(E_F), \quad (3)$$

where V_{scat} is the scattering potential and $N(E_F)$ is the density of scattering states at E_F . In the alloys investigated here, V_{scat} is nearly constant due to the small difference of atomic number between Fe and Co and $N(E_F) \sim N_{3d}(E_F)$.¹

Combining Eqs. (1)–(3) shows the resistance in ferromagnetic 3d transition metal systems is related to the DOS of the majority, $N_{\uparrow 3d}(E_F)$, and the minority, $N_{\downarrow 3d}(E_F)$, 3d bands at E_F

$$\rho = c \cdot \frac{N_{\uparrow 3d}(E_F) \cdot N_{\downarrow 3d}(E_F)}{N_{\uparrow 3d}(E_F) + N_{\downarrow 3d}(E_F)}, \quad (4)$$

where c is a constant related to V_{scat} . In Sec. III B, Eq. (4) will be applied to the rigid-band model of bcc Fe(Co) with reference to our experimental results.

B. Rigid-band model

We assume a rigid-band model where the DOS is (a) constant, (b) has a parabolic distribution, or (c) has a Gaussian distribution to fit experimental results.

1. Constant DOS (rectangular band)

The simplest rigid-band model considers a constant DOS in each composite d-band with a band width W_d , as shown in Fig. 3(a). The DOS can be expressed⁹

$$N_d(E) = \frac{5}{W_d} \text{ per atom, for } E_d - \frac{1}{2}W_d < E < E_d + \frac{1}{2}W_d;$$

$$N_d(E) = 0, \text{ otherwise,}$$

where E_d is the energy difference between the middle of the composite d-band and the lower band edge of the s-band.

The composition dependence of resistivity (ρ) and magnetic moment (M) are schematically shown in Fig. 3(b). We can see that the resistivity remains the same as that of Fe before the majority band is fully filled which occurs at around 44 at. % of Co. After that, the system becomes a strong ferromagnet and the resistivity suddenly drops. It is worth mentioning that the resistivity drops to zero if using

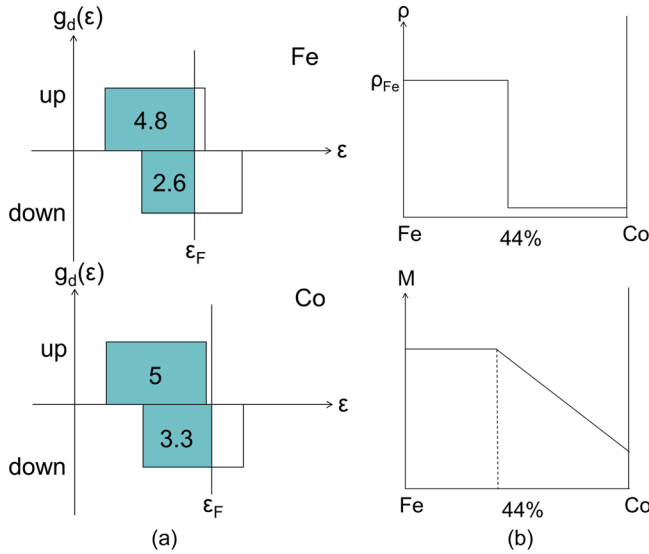


FIG. 3. (a) DOS for the rectangular rigid-band model of Fe and Co, (b) composition dependence of resistivity and magnetic moment in FeCo alloys for rectangular bands.

Eq. (4). In reality, there should be a very small amount of unoccupied states left at E_F which still enable some scattering events of majority electrons. Thus, in Fig. 3(b), the s-d scattering contribution of resistivity drops to a very low value instead of zero.

Similar to resistivity, the magnetic moment remains the same as that of Fe before the majority band is fully filled which occurs at around 44 at. % of Co. After that, the system becomes a strong ferromagnet and the magnetic moment drops with a slope of -1 as illustrated in Fig. 3(b).

2. Parabolic DOS

When the band shape is simplified as parabolic, Fig. 4(a), the composition dependence of resistivity and mag-

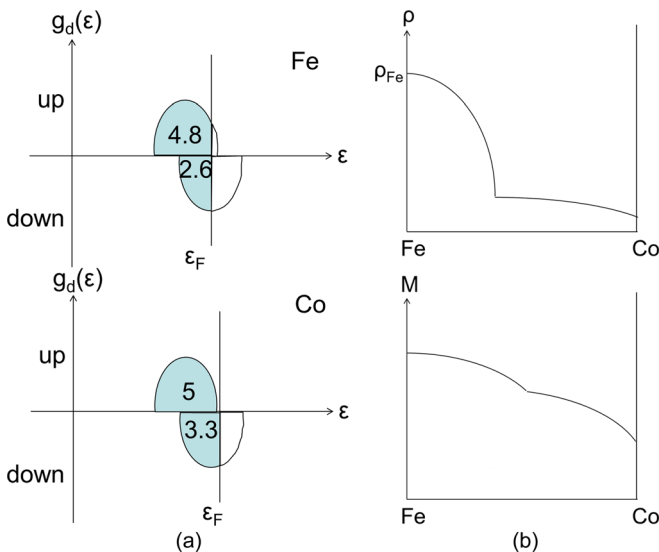


FIG. 4. (a) DOS for the parabolic rigid-band model of Fe and Co, (b) composition dependence of resistivity and magnetic moment in FeCo alloys for parabolic bands.

netic moment are shown in Fig. 4(b). Unlike the rectangular band shape, a parabolic band shape results in smooth DOS. However, neither the resistivity nor the magnetic moment maximum with Co substitution for Fe is adequately simulated.

3. Gaussian distributed DOS

A better estimate of the actual band structure can be obtained by fitting it to several Gaussian peaks. The locations and shapes of the peaks and E_F assumed here were based on the calculated band structures of bcc Fe(Co) alloys by Schwarz *et al.*¹⁰ as reproduced in Figs. 5(a) and 5(b). Other calculations on crystalline Fe(Co) alloying system with similar locations and shapes of the peaks have been reported in Refs. 11 and 12. The electronic structure calculations for FeB¹³ and CoB¹⁴ amorphous alloys

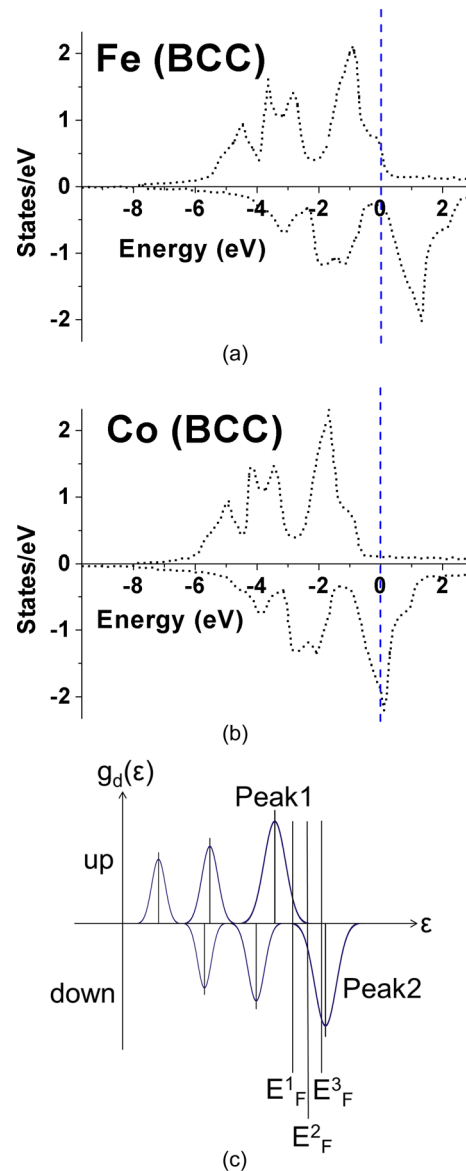


FIG. 5. Majority and minority DOS (a) for calculated bcc Fe, (b) for calculated bcc Co and, (c) simplified by Gaussian distributed DOS (the locations of E_F 's for bcc Fe (E_F^1), $Fe_{50}Co_{50}$ (E_F^2), and Co (E_F^3) are labeled).¹⁰

provide evidence that the DOS can be approximated by Gaussian distributed peaks in Fe(Co)-based amorphous systems.

Fig. 5(c) schematically demonstrates the simplified band distribution by Gaussian peaks and the locations of E_F 's for bcc Fe (E_F^1), bcc Fe₅₀Co₅₀ (E_F^2), and hypothetical bcc Co (E_F^3). Since the smaller resistance is always dominant in a parallel circuit as shown in Fig. 2, the resistivity maximum in the FeCo alloying system can be qualitatively predicted based on Fig. 5(c). We can see that the main peak (labeled Peak 1) of the spin-up band and the main peak (labeled Peak 2) of the spin-down band are responsible for the density of 3d states at E_F for bcc Fe(Co) alloys. The E_F of pure Fe locates relatively closer to Peak 1 so the smaller resistivity of spin-down channel is dominant. On the contrary, the E_F of either pure Co or Fe₅₀Co₅₀ locates relatively closer to Peak 2 so the smaller resistivity of spin-up channel is dominant. The maximum resistivity should be achieved by a composition in the Fe-rich region whose E_F locates right in the middle of

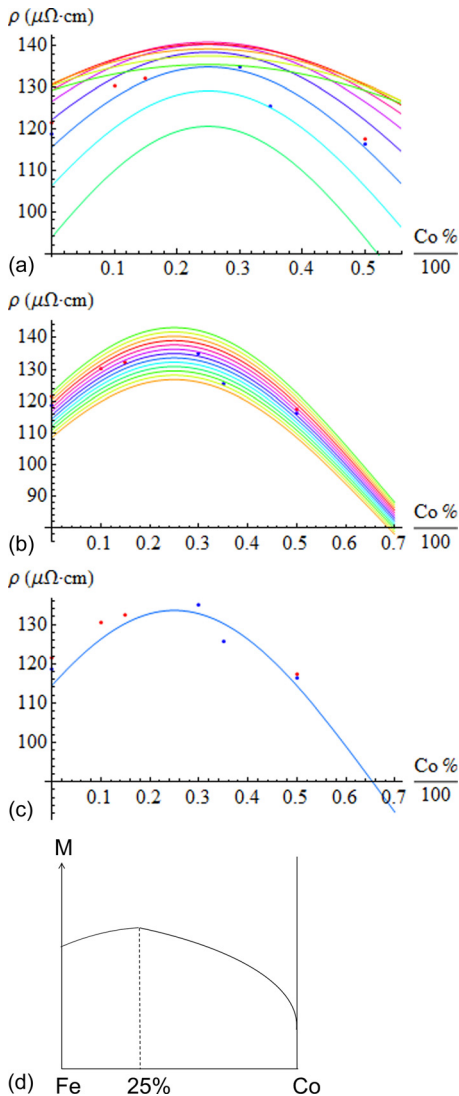


FIG. 6. Fits of the composition dependence of resistivity to experimental data with (a) $c = 990$ and variable σ in the range of 0.45–1.05, (b) $\sigma = 0.7$ and variable c in the range of 930–1050, (c) $c = 990$ and $\sigma = 0.7$, (d) composition dependence of magnetic moment for Gaussian DOS.

Peak 1 and Peak 2. In other words, the resistivity maximum in the Fe-rich region is a logical result of the fact that the E_F of bcc Fe locates at a valley of the minority spin band between two peaks.

The composition dependence of resistivity was simulated by *Mathematica 7.0* and fit to experimental data. In the fitting process, there are two variable parameters: the standard deviation σ of the Gaussian peaks and the constant c in Eq. (4) which is related to V_{scat} . As shown in Figure 6(a), the resistivity curve becomes flatter with increasing σ . As shown in Fig. 6(b), the resistivity curve shifts upward with increasing c . The empirically determined best fit to our experimental data is shown in Fig. 6(c) with $\sigma = 0.7$ and $c = 990$. Although the specific shape and location of this resistivity curve is variable, we can see that the maximum is always achieved by the composition of around 25 at. % Co because it is physically determined by the locations of Peak 1 and Peak 2 in Fig. 5(c).

The composition dependence of magnetic moment is schematically shown in Fig. 6(d). The magnetic moment also reaches a maximum at around 25 at. % Co. Beyond this Co content, however, it does not decrease as fast as resistivity because the magnetic moment is related to the total numbers of majority and minority electrons below E_F instead of the density of 3d states at E_F .

IV. CONCLUSIONS

In conclusion, we demonstrate experimental results for the composition dependence of the room temperature resistivity of amorphous $(\text{Fe}_{100-x}\text{Co}_x)_{89-y}\text{Zr}_7\text{B}_4\text{Cu}_y$ ($0 \leq x \leq 50$, $y = 0, 1$) alloys in this work. The relatively high Curie temperatures of these alloys indicate that the two-current model originally proposed by Mott for crystalline ferromagnetic transition metals can be extended to this amorphous disordered system. To model the composition dependence of resistivity and magnetic moment which are related to the band structure of bcc Fe(Co), the rigid-band assumption is made considering the small difference in atomic number between Fe and Co. Three models for the shape of the rigid-band were investigated and only the Gaussian distributed DOS was found to be sufficient to simulate both the resistivity maximum and the magnetic moment maximum in the Fe-rich region. The work presented here can potentially guide development of HITPERM alloys for high frequency applications.¹⁵

ACKNOWLEDGMENTS

This work was supported by the ARL through Grant No. W911NF-08-2-0024 and ARPA-E through Grant No. DE-FOA-0000474.

¹N. F. Mott, *Adv. Phys.* **13**, 325 (1964).

²A. P. Malozemoff, *Phys. Rev. B* **32**, 6080 (1985).

³M. E. McHenry, J. M. MacLaren, and D. P. Clougherty, *J. Appl. Phys.* **70**, 5932 (1991).

⁴J. Friedel, *Nuovo Cimento, Suppl.* **7**, 287 (1958).

⁵M. E. McHenry, M. A. Willard, and D. E. Laughlin, *Prog. Mater. Sci.* **44**, 291 (1999).

- ⁶S. Shen, P. R. Ohodnicki, S. J. Kernion, A. Leary, V. Keylin, J. F. Huth, and M. E. McHenry, in *Energy Technology 2012: Carbon Dioxide Management and Other Technologies, Orlando* (John Wiley & Sons, Inc. 2012), p. 275.
- ⁷P. V. Paluskar, J. J. Attema, G. A. de Wijs, S. Fiddy, E. Snoeck, J. T. Kohlhepp, H. J. M. Swagten, R. A. de Groot, and B. Koopmans, *Phys. Rev. Lett.* **100**, 057205 (2008).
- ⁸F. P. Beitel and E. M. Pugh, *Phys. Rev.* **112**, 1516 (1958).
- ⁹E. Economou, *The Physics of Solids, Essentials and Beyond* (Springer-Verlag, Heidelberg, 2010).
- ¹⁰K. Schwarz, P. Mohn, P. Blaha, and J. Kübler, *J. Phys. F: Met. Phys.* **14**, 2659 (1984).
- ¹¹V. L. Moruzzi, J. F. Janak, and A. R. Williams, *Calculated Electronic Properties of Metals* (Pergamon, New York, 1978).
- ¹²J. M. MacLaren, T. C. Schulthess, W. H. Butler, R. Sutton, and M. E. McHenry, *J. Appl. Phys.* **85**, 4833 (1999).
- ¹³J. Hafner, M. Tegze, and Ch. Becker, *Phys. Rev. B* **49**, 285 (1994).
- ¹⁴H. Tanaka and S. Takayama, *Phys. Rev. B* **47**, 2671 (1993).
- ¹⁵A. Leary, P. R. Ohodnicki, and M. E. McHenry, *JOM* **64**, 772 (2012).